http://dx.doi.org/10.5012/bkcs.2012.33.1.322

Docking and Molecular Dynamics Simulations of Celastrol Binding to p23

Sanghwa Han

Department of Biochemistry and Institute for Life Sciences, Kangwon National University, Chunchon 200-701, Korea
**E-mail: hansh@kangwon.ac.kr*
Received November 4, 2011, Accepted November 9, 2011

Key Words : Celastrol, p23, Pocking, Molecular dynamics

Celastrol (CSL), a quinone methide triterpenoid (Fig. 1(a)) from thunder god vine, is a natural product with high *anti*-inflammatory and *anti*-cancer potential.[1] One of CSL's major targets is the Hsp90 chaperoning system and its inhibition by CSL results in destabilization of the Hsp90 client proteins involved in inflammation and cancer. Early reports suggest that CSL binds to the N-terminal domain of Hsp90 to interfere with the Hsp90-Cdc37 association.[2] Later it was demonstrated that CSL reacts with cysteine residues of Cdc37 causing aggregation of Cdc37.[3] Recently Chadli *et al.*[4] showed that CSL induces fibrillization of p23, an Hsp90 co-chaperone that is specific for steroid receptors. Although CSL can react with cysteine residues of p23, non-covalent association is implicated in the fibrillization because reduced CSL is equally effective. The authors identified the amino acid residues whose NMR signals were perturbed upon CSL-COO^- binding. Structure of the p23-CSL complex has not been determined, however. We previously performed docking and molecular dynamics simulations to identify the CSL binding site of Erk2 and found that CSL inhibits FceRI signaling by blocking the Erk2's ATP binding site.[5] A similar strategy was employed in this study to model the structure of the p23-CSL complex.

We first started by locating the possible binding site(s) by performing blind docking simulations on four CSL variants, namely oxidized (CSL) and reduced (H_2CSL) with protonated (-COOH) and deprotonated carboxy (-COO^-) group. All the atoms in the protein including side chains were treated rigid. Autodock 4.2 was used with the Lamarckian genetic algorithm. When the docked conformations of CSL-COO^- were clustered with 0.1 nm RMSD, 81 out of 100 conformations were clustered with the lowest energy conformation. Five other binding sites had a very low population. Inhibition constant, K_i, was 186 nM demonstrating a tight association of CSL-COO^- with p23. Other CSL's also showed high probability (74% for CSL-COOH, 65% for H_2CSL-COO^-, and 61% for H_2CSL-COOH) of docking in the lowest energy conformation. Inhibition constants were also very small ranging from 131 to 226 nM.

Structures of the lowest energy conformations of p23-CSL complexes are shown in Figure 1(b). All four CSL's docked in the same site on p23 with the same orientation. The Doolittle-Kyte hydrophobicity surface shows that the central hydrocarbon moiety of CSL is located in a hydrophobic area. The carboxy group of CSL-COO^- was locked into the position by forming hydrogen bonds with the amide hydrogens of Leu89, Thr90, and Ala94. It was also hydrogen bonded to hydroxy group of Thr90. In fact an analysis of binding energetics showed that the electrostatic contribution was much smaller than the van der Waals interaction and hydrogen bonding (data not shown). We can conclude that the docked structure is reasonable in a chemical sense considering that an unrealistic rigid protein structure was used in the docking simulations.

Molecular dynamics (MD) simulation is often employed for the refinement of a structure obtained from a docking

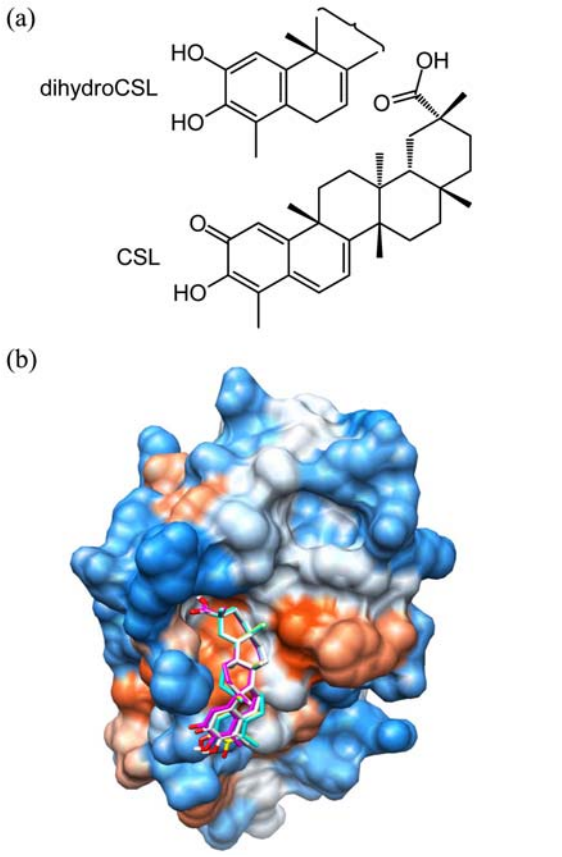

Figure 1. (a) Structure of celastrol (CSL) and its reduced form (dihydroCSL). (b) Docked structures of CSL-COO^- (gray), CSL-COOH (magenta), H_2CSL-COO^- (cyan), and H_2CSL-COOH (yellow). Colors of the protein surface represent the Doolittle-Kyte hydrophobicity scale (red for hydrophobic and blue for hydrophilic residues).

simulation. In MD simulation, the side chains are allowed to move and an energetically favorable structure can be obtained. Using GROMOS 43a1 force filed we carried out three independent runs of 20 ns MD simulation on the p23-CSL-COO^- complex. Due to low pK_a of the carboxy group, CSL is likely in the deprotonated state when bound to p23. A representative result is described below.

The structure of the lowest energy conformation obtained from docking simulation was used as the starting structure for MD simulation. The structure was immersed in water and its energy was minimized. After a short equilibration step, a production MD simulation was carried out for 20 ns. The RMSD trace of the system was stabilized soon after the start of MD simulation (not shown). To obtain a refined structure, the structures from MD simulation were averaged over the time period from 980 to 1000 ps (1 ns structure) and from 19980 to 20000 ps (20 ns structure). The resulting structures were further subjected to energy minimization. These two structures are compared in Figure 2(a). CSL-COO^- binding did not cause a major perturbation in the overall protein backbone except the loop region where the ligand was bound. Interestingly the guanidino group of Arg88 moved over toward the carboxy group of CSL-COO^- and formed hydrogen bonds with the latter. At the same time the ligand itself moved upward with a concomitant widening of the loop. To monitor the movement of Arg88 and the ligand as a function of time, we measured the distance between H_ε of Arg88 and carboxy O of CSL-COO^- (red dotted line) and the distance between hydroxy O of CSL-COO^- and C_α of Ser100. As shown in Figure 2(b), the guanidino group moved in toward the carboxy group of CSL-COO^- at ~5 ns. Simultaneously the ligand moved upward. The structure that was formed at 5 ns stayed stable thereafter. Participation of Arg88 in hydrogen bonding and concomitant movement of the ligand were consistently observed in three independent runs of MD simulations although the onset time varied among simulations.

The refined 20 ns structure in Figure 3(a) shows that CSL-

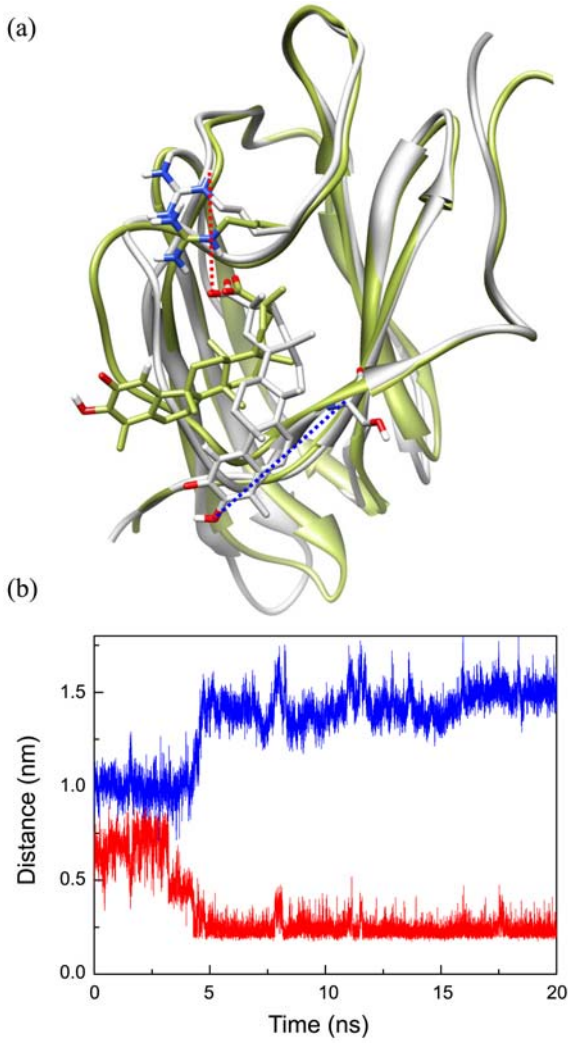

Figure 2. (a) Structures of p23-CSL-COO^- complex after 1 ns (gray) and 20 ns (green) of MD simulation. Each structure was averaged for 20 ps and subjected to a short energy minimization. Also shown are the distance between H_ε of Arg88 and carboxyl O of CSL-COO^- (red dotted line) and the distance between hydroxyl O of CSL-COO^- and C_α of Ser100 (blue dotted line). (b) Time evolution of the distances defined in Figure 2(a).

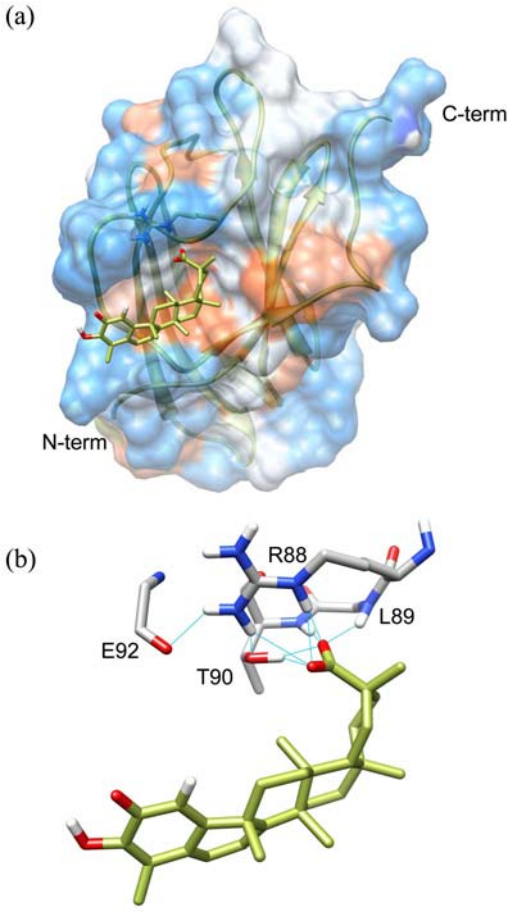

Figure 3. Structure of p23-CSL-COO^- complex after 20 ns of MD simulation. (a) CSL-COO^- is bound to a hydrophobic pocket on p23. Colors of the protein surface represent the Doolittle-Kyte hydrophobicity scale (see Fig. 1). (b) Hydrogen bonding network (cyan lines) around the carboxy group of bound CSL-COO^-. The structures in Figures 1, 2 and 3 were matched using MatchMaker tool of Chimera.

COO^- binds close to a loop near the C-terminal. Protein surface colored by the Doolittle-Kyte hydrophobicity scale demonstrates that the hydrocarbon moiety resides in the hydrophobic pocket which is composed mainly of Leu89, Leu96, and Leu99. Throughout the MD simulations no water molecules were found between the bound ligand and the protein surface due to a highly hydrophobic environment at the interface. This ensures a favorable van der Waals interaction between the ligand and the protein. In addition CSL-COO^- is located far from the two completely exposed cysteine residues suggesting that the complex formation is not a prerequisite for the previously reported covalent modification of a cysteine by CSL-COO^-.[4]

A close examination of the structure around the carboxy group of CSL-COO^- reveals an extensive network of hydrogen bonding. As shown in Figure 3(b), Arg88 and Thr90 play a pivotal role in anchoring the ligand. The guanidino group of Arg88 was locked in by hydrogen bonding with the amide O of Lys92 and hydroxy O of Thr90. This enabled the guanidino group to form hydrogen bonds with the carboxy O atoms of the ligand. The carboxy group was further stabilized by hydrogen bonding with hydroxy group of Thr90 and amide H of Leu89. This hydrogen bonding network fixes the position of CSL-COO^- in such a way that the hydrocarbon rings of the ligand fits in the hydrophobic pocket. The other end of CSL-COO^- is hydrophilic with a hydroxy group and sticks out to aqueous environment.

In summary, blind docking simulations identified a binding site of CSL-COO^- on p23. Further structural refinement by MD simulations revealed an extensive hydrogen bonding network between the ligand and nearby residues including Arg88 and Thr90. Hydrophobic interaction is implied between the hydrocarbon skeleton and the hydrophobic surface of the protein. The complex stayed stable during 20 ns of MD simulation suggesting that the binding is strong in both docking and MD simulations.

Experimental Section

Docking Simulation. Coordinates of four structures, oxidized (CSL) and reduced CSL (H_2CSL) with the protonated (-COOH) and deprotonated carboxy group (COO^-), were obtained from PRODRG (http://davapc1.bioch.dundee.ac.uk/prodrg).[6] These structures were subjected to geometry optimization at the level of HF/6-31G* using Gaussian 09. A good starting structure was important for a successful docking simulation. To ensure a blind docking we next set up a grid box (grid spacing 0.0375 nm) that was large enough to encompass the whole protein (1ejf.pdb). Gasteiger charges were used for both protein and ligand. Other charges, e.g. RESP for the ligand and Amber for the protein, did not produce good clustering. Using the Lamarckian genetic algorithm, a triplicate of 100 docking simulations were carried out for each CSL.

Molecular Dynamics Simulation. To refine the docked structure and examine its stability, we next performed molecular dynamics (MD) simulations using the GROMACS 4.0.7 software.[7] The coordinates of a docked ligand were extracted and submitted to PRODRG[6] to obtain the topology for the GROMOS 43a1 force field. Atomic charges in the topology obtained from PRODRG are often unreasonable[8] and therefore they were replaced by the Gasteiger charges that were used in the docking simulation. Charge groups were reassigned as suggested by the original developer of the force field. Similar results were obtained when charges were assigned by consulting the rtp file of the GROMOS 43a1 force field. The protein-ligand complex was then immersed in a SPC/E water box of cubic shape whose edges were placed at 1 nm from the protein. The system was electrically neutralized by adding a Na^+ ion. Particle mesh Ewald method[9] was used in the calculation of electrostatic energy. Cutoff distances for the Coulomb and van der Waals interactions were 1.0 and 1.4 nm, respectively. After a short energy minimization step using a steepest descent method, the system was subjected to equilibration at 300 K and 1 bar for 50 ps under the conditions of position restraints for heavy atoms and LINCS constraints[10] for all bonds. The system was coupled to the external bath by the velocity rescale thermostat[11] and the Parrinello-Rahman barostat.[12] Finally the position restraints were removed in the production MD calculations keeping all the other conditions unaltered. Analyses of the results were carried out using the GROMACS utility and Chimera.[13]

References

1. Kannaiyan, R.; Shanmugam, M. K.; Sethi, G. *Cancer Lett.* **2011**, *303*, 9.
2. Hieronymus, H.; Lamb, J.; Ross, K. N.; Peng, X. P.; Clement, C.; Rodina, A.; Nieto, M.; Du, J.; Stegmaier, K.; Raj, S. M.; Maloney, K. N.; Clardy, J.; Hahn, W. C.; Chiosis, G.; Golub, T. R. *Cancer Cell* **2006**, *10*, 321.
3. Sreeramulu, Sv; Gande, S. L.; Göbel, M.; Schwalbe, H. *Angew. Chem. Int. Ed.* **2009**, *48*, 5853.
4. Chadli, A.; Felts, S. J.; Wang, Q.; Sullivan, W. P.; Botuyan, M. V.; Fauq, A.; Ramirez-Alvarado, M.; Mer, G. *J. Biol. Chem.* **2010**, *285*, 4224.
5. Kim, Y.; Kim, K.; Lee, H.; Han, S.; Lee, Y. S.; Choe, J.; Kim, Y. M.; Hahn, J. H.; Ro, J. Y.; Jeoung, D. *Eur. J. Pharmacol.* **2009**, *612*, 131.
6. Schüttelkopf, A. W.; van Aalten, D. M. F. *Acta Crystallogr.* **2004**, *D60*, 1355.
7. van Der Spoel, D.; Lindahl, E.; Hess, B.; Groenhof, G.; Mark, A. E.; Berendsen, H. J. *J. Comput. Chem.* **2005**, *26*, 1701.
8. Lemkul, J. A.; Allen, W. J.; Bevan, D. R. *J. Chem. Inf. Model* **2010**, *50*, 2221.
9. Essmann, U.; Perera, L.; Berkowitz, M. L.; Darden, T.; Lee, H.; Pedersen, L. G. *J. Chem. Phys.* **1995**, *103*, 8577.
10. Hess, B.; Bekker, H.; Berendsen, H. J. C.; Fraaije, J. G. E. M. *J. Comput. Chem.* **1997**, *18*, 1463.
11. Bussi, G.; Donadio, D.; Parrinello, M. *J. Chem. Phys.* **2007**, *126*, 014101.
12. Parrinello, M.; Rahman, A. *J. Chem. Phys.* **1982**, *76*, 2662.
13. Pettersen, E. F.; Goddard, T. D.; Huang, C. C.; Couch, G. S.; Greenblatt, D. M.; Meng, E. C.; Ferrin, T. E. *J. Comput. Chem.* **2004**, *25*, 1605.